ECCI and EBSD Study of Subsurface Damages in High Speed Turning of Inconel 718 under Different Tools and Machining Parameters

Zhe Chen[1,*], Ru Lin Peng[1], Jinming Zhou[2], Johan Moverare[1], Volodymyr Bushlya[2], Sten Johansson[1]

[1] Division of Engineering Materials, Linköping University, 58183 Linköping, Sweden
[2] Division of Production and Materials Engineering, Lund University, 22100 Lund, Sweden
* Corresponding author: zhe.chen@liu.se

Abstract Inconel 718 is a Ni-based superalloy that can perform excellently at elevated temperatures. However, surface and subsurface damages in the form of microstructural and property changes and tensile residual stresses are common in a machined Inconel 718 component because of its poor machinability. Such damages have a significant influence on performance and the life time of the part. To characterise microstructural damages and understand how they are correlated to machining conditions are not only important for the evaluation of surface integrity but also for the optimization of machining operations to minimise effects from the machining process. This paper uses the ECCI (electron channelling contrast imaging) and EBSD (electron back scatter diffraction) methods to study the effect of cutting tools and cutting speeds on subsurface plastic deformation of machined Inconel 718. When turning at 200 m/min, a comparable level of plastic deformation was found under the surface machined with uncoated cubic boron nitride (CBN), titanium nitride coated CBN and whisker reinforced alumina (WRA). With an increase in cutting speed, the plastic deformation depth increased, and uncoated CBN tools showed superior performance in term of subsurface microstructure alterations compared to the other tool materials.

Keywords Inconel 718, High speed turning, Surface integrity, Plastic deformation, EBSD

1. Introduction

Superalloys which can maintain high performance at elevated temperatures are widely used in aerospace, automotive, and power industries. Ni-based superalloys are outstanding members in this big family because of their high resistance to corrosion, mechanical and thermal fatigue, mechanical and thermal shock, and creep at high temperatures [1, 2]. However, Ni-based superalloys are difficult-to-cut materials due to their superior mechanical properties and the low thermal conductivity. High cutting heat tends to generate in the contact area between cutting tools and the component during machining processes. The high temperature which can be in excess of 1200 °C leads to rapid tool wear because of softening of tool materials [3, 4]. These characterizations consequently result in surface damages, and eventually affect the mechanical performance and service life of final products. In industries, the finish machining of Ni-based superalloys is generally performed by using traditional cemented carbide tools at low cutting speeds (30-90 m/min) to maintain a reasonable tool life [5]. However, in recent years, more aggressive cutting conditions, such as higher cutting speeds, are promoted for the purpose of increasing production efficiency and reducing manufacturing costs. These accelerate the application of new tool materials like whisker reinforced ceramics (WRC) and cubic boron nitride (CBN) [3, 6, 7]. WRC tools can maintain a high hardness at elevated temperatures and the toughness is dramatically improved by adding whiskers of silicon carbides. The achievable cutting speed varies from 200 m/min to 750 m/min, depending

on the hardness of the superalloy [8]. Compared to WRC tools, CBN tools have a better strength and resistance to fracture but poorer chemical stability [7, 8]. By applying coatings, a diffusion barrier forms which can suppress the chemical wear of CBN tools [9].

During high speed machining operations, the alloy will be exposed to high thermal and mechanical fields which can lead to microstructure alterations near the surface, such as plastic deformation, phase transformation and recrystallization [10-12]. These alterations play a significant role in determining the final fatigue strength of the machined component [13]. Therefore, the surface integrity provided by using these novel machining tools should be investigated in order to predict the quality of machined components. The aim of this study is to evaluate and compare microstructure alterations with focus on the plastic deformation under the machined surface produced with uncoated CBN, coated CBN and WRC tools at high cutting speeds.

2. Experimental details

Solution annealed and aged Inconel 718 with 45HRC hardness was chosen for this study. The chemical composition is given in Table 1. A bar with 70 mm diameter and 200 mm in length was machined at finishing turning conditions. Cutting tools consisted of uncoated CBN (UCBN), titanium nitride-coated CBN (CCBN) and whisker reinforced alumina (WRA). UCBN and CCBN tools have low CBN contents (approximately 50% vol.). The thickness of the titanium nitride coating was 2 μm. Whisker reinforced alumina inserts with honed cutting edge and 0.1×20° chamfer were employed. The insert was mounted in the tool holder provided 6° inclination and -6° rake angle. Coolant was used throughout all cutting tests. Two cutting speeds, v_c =200 m/min and 350 m/min, were selected. The cutting feed rate f =0.1 mm/rev and the cutting depth a_p =0.3 mm, were constant for all tests. Cutting forces in the cutting, feed and radial directions were measured with a force dynamometer, Kistler 9121.

Table 1. Chemical composition (wt. %) of Inconel 718

Ni	Cr	Nb	Mo	Ti	Al	C	Si	Fe
53.8	18.1	5.5	2.9	1	0.55	0.25	0.04	Balance

The ECCI (electron channelling contrast imaging) technique is based on variations of the collected backscattered electrons intensity, and observed channelling contrast is attributed to lattice misorientations introduced during fabrication or deformation processes [14]. The EBSD (electron back scatter diffraction) technique can be used to quantitatively measure the extent of plastic deformation beneath the machined surface by offering grain orientations as well as information about intragranular misorientations [15]. In this study, ECCI and EBSD techniques were used to characterize microstructure and measure the deformation intensity and depth. All these studies were conducted on a Hitachi SU-70 FED electron scanning microscope installed with an EBSD set-up. Results of the density of low angle grain boundaries were obtained using the Channel-5 software from HKL technology.

3. Results and discussions

3.1 Subsurface microstructure

Typical microstructure alterations introduced during the machining process are presented in Fig. 1a. Based on the observed morphology, four obvious zones can be identified in the machined subsurface region [16]. The very thin layer (less than 1 μm) close to the top surface is the heat affected zone. The microstructure was strongly affected by the heat generated during the cutting process, as a consequence of the high cutting speed. The high resolution image shows that the structure in the heat affected zone is highly refined with nano-scaled grain size which is much smaller than the grain size of the bulk material (Fig.1b). This ultrafine nanostructure corresponds to the white layer often found after high speed cutting [17]. The formation of the white layer is generally attributed to a high cutting temperature followed by rapid cooling or severe plastic deformation [18]. Beneath the heat affected zone, the severe deformation can be characterized by bending and elongation of grains, grain boundaries and slip bands towards the cutting direction. This morphology varies as the depth increases. In the slight deformation zone, only some slip bands can be observed. The intensity of the plastic deformation declines following the temperature and mechanical load gradient from the surface to the bulk material.

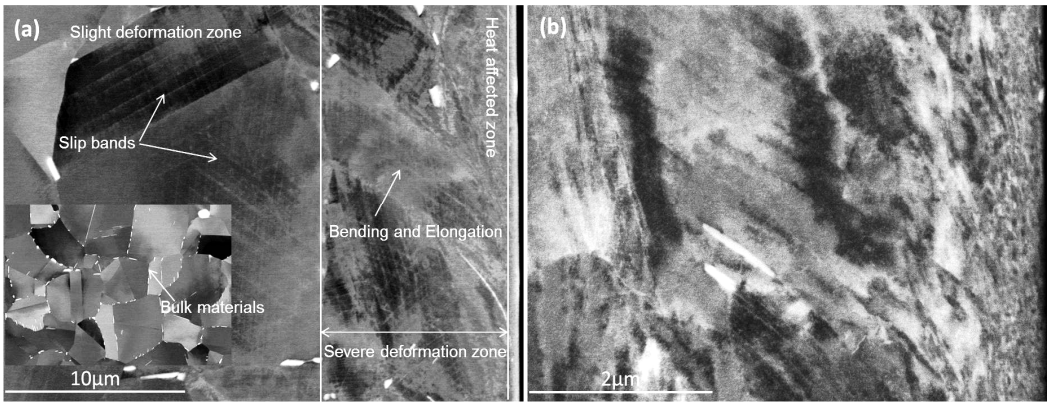

Figure 1. Typical microstructure of (a) machined surface and subsurface layers (b) the heat affected zone (CCBN tools, 350 m/min)

Figs. 2a and b show the effect of cutting speeds on the plastic deformation beneath the surface machined with WRA tools. When the cutting speed was increased from 200 m/min to 350 m/min, more distinguishable bending and slip bands were observed and the whole deformation area in the subsurface layer became much larger. Since the cutting force components of WRA tools were found to slightly decrease with the increased cutting speed (Fig. 3a), it may be concluded that the increased cutting temperature at the higher cutting speed is responsible for the greater level of the plastic deformation in the subsurface zone [19]. The same influence of cutting speeds was observed in the machined surface produced by UCBN tools and CCBN tools (Fig. 2c-f). Besides cutting speeds, the type of cutting tools is also an essential parameter affecting the plastic deformation in the machined subsurface. At 350 m/min, the most severe and deeper plastic deformation was found in the subsurface machined with WRA tools (Fig. 2b). It was also found that cutting with CCBN

tools resulted in a larger extent of plastic deformation in the machined subsurface compared with UCBN tools (Figs. 2d and f). These observed differences in the plastic deformation level can be explained by the increased cutting forces (Fig. 3b). The highest force level found for WRA tools leads to the largest plastic deformation under the machined surface. For the case of CBN tools, the higher cutting forces given by CCBN tools are responsible for the greater level of subsurface plastic deformation. It is expected that CCBN tools should show a lower cutting force than UCBN tools due to a lower friction coefficient and thermal conductivity of the titanium nitride coatings [20]. The opposite result is mainly due to the different tool microgeometry. Simulation and experimental results indicated that cutting forces increase as the tool radius increases [21, 22]. In this study, the edge radius r_β is 15-18 μm for UCBN tools, 20-22 μm for CCBN tools, 25-28 μm for WRA tools. At the higher cutting speed, the cutting tools had a strong influence on the subsurface plastic deformation level. However, when cutting at 200 m/min, comparable plastic deformation was found in Figs. 2a, c and e, and no obvious differences can be distinguished in the microstructure images for the different tools.

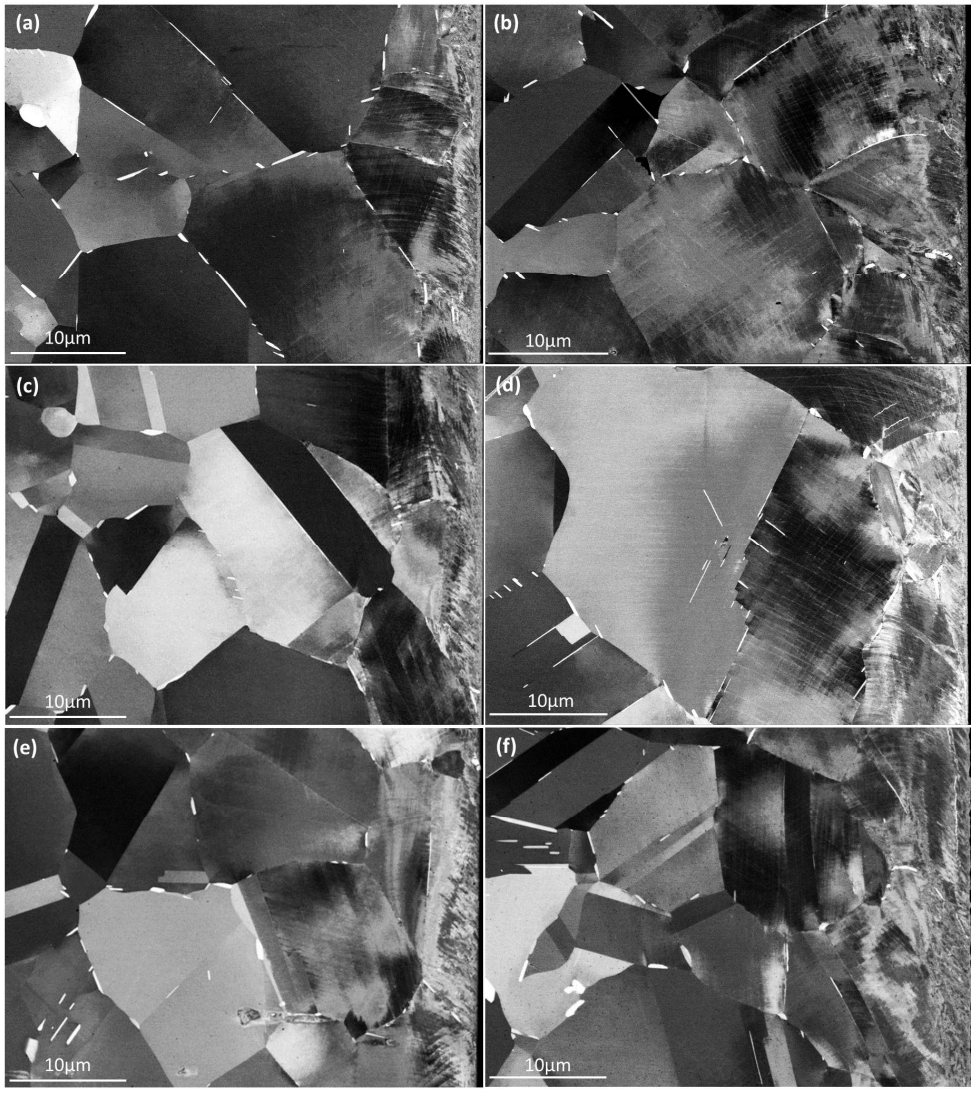

Figure 2. Microstructure images showing surface and subsurface deformation (loaded on the right side)
(a) WRA tools, v_c =200 m/min (b) WRA tools, v_c =350 m/min (c) UCBN tools, v_c =200 m/min
(d) UCBN tools, v_c =350 m/min (e) CCBN tools, v_c=200 m/min (f) CCBN tools, v_c =350 m/min

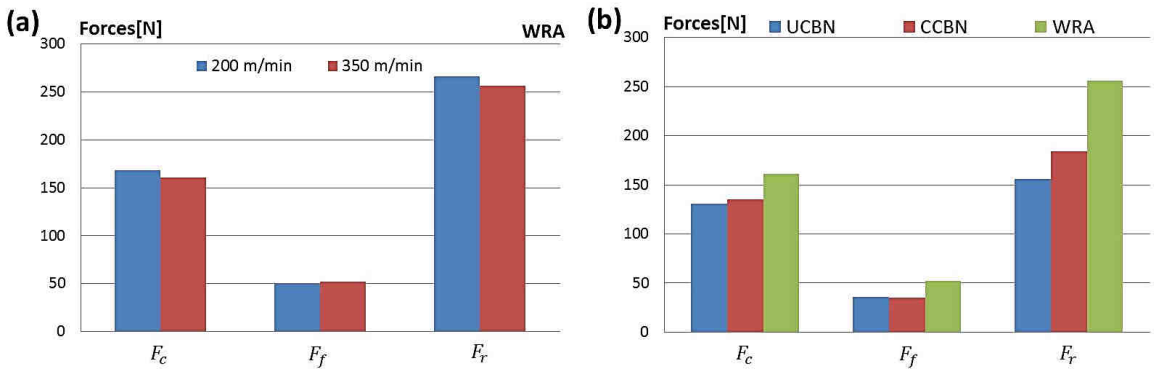

Figure 3. Comparison of cutting (F_c), feed (F_f) and radial (F_r) force components for (a) WRA tools, v_c=200 m/min and v_c=350 m/min (b) UCBN, CCBN and WRA tools, v_c=350 m/min

3.2 EBSD measurement

The EBSD maps were scanned with a step size of 1 μm in both vertical and horizontal direction from the surface. The crystallographic orientation of each measured point was collected according to the Kikuchi pattern and then the crystallographic misorientation associated with plastic deformation between each two points was calculated. A misorientation angle within the range of 1° and 10° was defined as a low angle grain boundary. The EBSD maps in Fig. 4 reveal the subsurface plastic deformation induced by turning using WRA tools. Areas where the value of the misorientation angle is within the range of 1° and 5° are marked by white lines, and those within the range of 5° and 10° are marked by red lines. The red lines were found to concentrate in the top surface showing a greater level of plastic deformation in this area. Meanwhile, when moving away from the surface into the bulk material, a general decrease of the white lines can be observed which shows the decrease of the plastic deformation. This tendency is corresponding to the microstructure variation from the heat affected zone to the undeformed zone. By calculating statistical data obtained in five random areas under the machined surface, misorientation variations versus the depth were delineated to demonstrate the plastic deformation level and depth beneath the machined surface (Fig. 4c). The increase of subsurface plastic deformation at the higher cutting speed was confirmed by the higher density and the greater depth of the misorientation. The EBSD results combined with the microstructure observation demonstrate that the higher cutting speed tends to result in a larger level of plastic deformation in the subsurface area

Microstructure observations in Section 3.1 have proven that the choice of cutting tools had an effect on the subsurface plastic deformation level, but this effect highly depends on the cutting speed. Fig. 5b confirmed the increase of plastic deformation for the machined surface from UCBN tools, CCBN tools and WRA tools at 350 m/min. This increase is strongly related to the increased cutting force level. However, at the lower cutting speed of 200 m/min, although the cutting forces for WRA tools still maintain the highest level compared with UCBN and CCBN tools (Fig. 5c), the plastic deformation generated during machining operations with WRA tools shows a slightly lower level instead (Fig. 5a). Such a significant change is probably attributed to the lower cutting temperature at a relatively low cutting speed. The coherency strain hardening has been reported to be the principal strengthening mechanism in aged Inconel 718 [23]. The major strengthening phase in Inconel 718 is

the γ'' phase. When the cutting temperature is below the γ'' solvus temperature, due to the strain hardening, the further plastic deformation is restricted. Therefore, at the lower cutting speed, the cutting forces had a limited effect on determining the plastic deformation in the machined subsurface. UCBN, CCBN and WRA tools give a similar plastic deformation level.

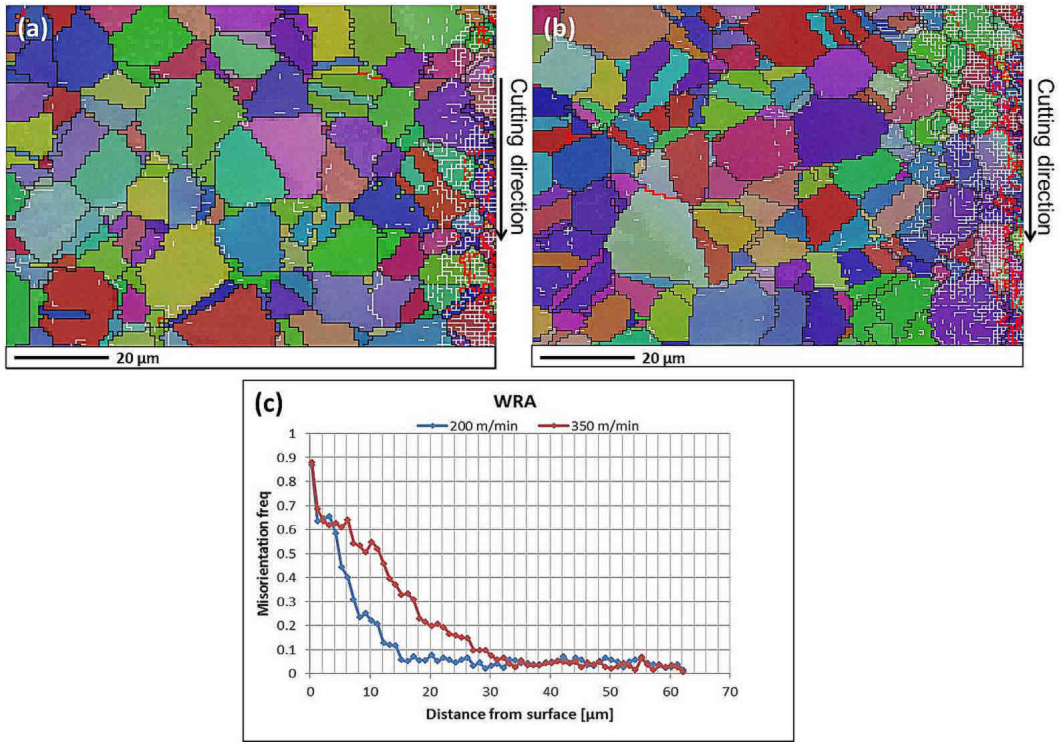

Figure 4. EBSD maps of subsurface deformation (a) WRA tools, v_c =200 m/min (b) WRA tools, v_c =350 m/min (c) Misorientation within grains beneath the surface machined with WRA tools

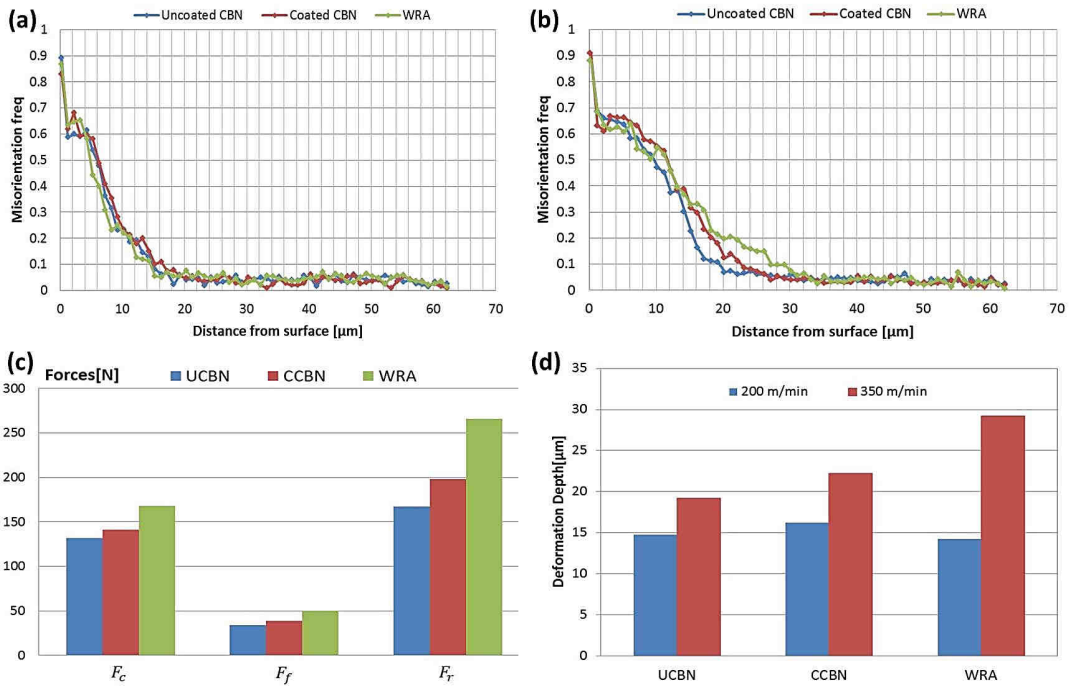

Figure 5. Misorientation within grains beneath the surface machined at (a) 200 m/min (b) 350 m/min (c) Cutting force components at 200 m/min (d) Deformation depth under different cutting conditions

Deformation depth is an essential parameter to assess the damage in form of structural alterations produced by mechanical machining processes. Fig. 5d summarises the influence of cutting conditions on the plastic deformation depth. It reveals that a higher cutting speed can significantly increase the plastic deformation depth under the machined surface. This tendency is more obvious for WRA tools, suggesting that the performance of WRA tools is much more sensitive to the cutting speed. Comparing the effect of the three cutting tools, the plastic deformation depth varies within a small range of 2-3 μm at the lower speed. However, when cutting at the higher speed, a noticeable increase of the deformation depth from UCBN tools, CCBN tools and WRA tools was found.

4. Conclusions

Microstructure alterations of Inconel 718 machined with UCBN, CCBN and WRA tools at two different cutting speeds have been investigated using ECCI and EBSD techniques. An attempt has been made to characterize the performance of the three advanced cutting tools in high speed machining in terms of influence on the subsurface microstructure. The results reveal an obvious alteration of subsurface microstructure associated with the gradient of mechanical forces and temperature along the depth direction for all the cutting conditions. The cutting speed was found to have a significant influence on subsurface plastic deformation with a larger plastic deformation level at higher cutting speeds. For the effect of cutting tools, comparable plastic deformation was observed under the surface machined with UCBN, CCBN and WRA tools at the lower cutting speed. However, at the higher cutting speed, the UCBN tools outperformed the other two types of cutting tools. Hence, for the cutting conditions studied in the current work, UCBN tools should be considered when a higher cutting speed is required in order to increase the production efficiency.

Acknowledgements

The authors of this paper express their sincere thanks to Mrs Annethe Billenius for her help with the sample preparation. The scholarship provided by the China Scholarship Council for Mr Zhe Chen is also greatly appreciated.

References

[1] E.O. Ezugwu, Key improvements in the machining of difficult-to-cut aerospace superalloys. Int. J. Mach. Tool Manuf., 45 (2005) 1353-1367.

[2] D. Ulutan, T. Ozel, Machining induced surface integrity in titanium and nickel alloys: A review. Int. J. Mach. Tool Manuf., 51 (2011) 250-280.

[3] T. Kitagawa, A. Kubo, K. Maekawa, Temperature and wear of cutting tools in high-speed machining of Inconel 718 and Ti6Al6V2Sn. Wear., 202 (1997) 142-148.

[4] F. Pusavec, H. Hamdi, J. Kopac, I. Jawahir, Surface integrity in cryogenic machining of nickel based alloy- Inconel 718. J. Mater. Process. Technol., 211 (2011) 773-783.

[5] R. M'Saoubi, T. Larsson, J. Outeiro, Y. Guo, S. Suslov, C. Saldana, S. Chandrasekar, Surface integrity analysis of machined Inconel 718 over multiple length scales. CIRP Ann. Manuf. Technol., 61 (2012) 99-102.

[6] R. Arunachalam, M.A. Mannan, Machinability of nickel-based high temperature alloys. Mach. Sci. Technol., 4 (2000) 127-168.

[7] J.P. Costes, Y. Guillet, G. Poulachon, M. Dessoly, Tool-life and wear mechanisms of CBN tools in machining of Inconel 718. J. Mach. Tool Manuf., 47 (2007) 1081-1087.

[8] I.A. Choudhury, M.A. El-Baradie, Machinability of nickel-base super alloys: a general review. J. Mater. Process. Technol., 77 (1998) 278-284.

[9] S.A. Khan, S.L. Soo, D.K. Aspinwall, C. Sage, P. Harden, M. Fleming, A. White, R. M'Saoubi, Tool wear/life evaluation when finish turning Inconel 718 using PCBN tooling. Procedia CIRP, 1 (2012) 283-288.

[10] D.G. Thakur, B. Ramamoorthy, L. Vijayaraghavan, Machinability investigation of Inconel 718 in high-speed turning. Int. J. Adv. Manuf. Technol., 45 (2009) 421-429.

[11] M. Imran, P.T. Mativenga, S. Kannan, Evaluation of the effects of tool geometry on tool wear and surface integrity in the micro drilling process for Inconel 718 alloy. Int. J. Mach. Mach. Mater., 11 (2012) 244-262.

[12] J. Li, M. Umemoto, Y. Todaka, K. Tsuchiya, A microstructural investigation of the surface of a drilled hole in carbon steels. Acta Mater., 55 (2007) 1397-1406.

[13] D. Novovic, R.C. Dewes, D.K. Aspinwall, W. Voice, P. Bowen, The effect of machined topography and integrity on fatigue life. Int. J. Mach. Tool Manuf., 44 (2004) 125-134.

[14] S. Kaboli, J. Su, R. Gauvin, Comparison of electron channeling contrast imaging (ECCI) and electron back scattered diffraction (EBSD) using Hitachi SU8000 FE-SEM. Microsc. Microanal., 18 (2012) 700-701.

[15] R. M'Saoubi, L. Ryde, Application of the EBSD technique for the characterisation of deformation zones in metal cutting. Mater. Sci. Eng. A, 405 (2005) 339-349.

[16] J.M. Zhou, V. Bushlya, R.L. Peng, S. Johansson, P. Avdovic, J. Stahl, Effects of tool wear on subsurface deformation of nickel-based superalloy. Procedia Eng., 19 (2011) 407-413.

[17] S. Veldhuis, G. Dosbaeva, A. Elfizy, G. Fox-Rabinovich, T. Wagg, Investigations of white layer formation during machining of powder metallurgical Ni-based ME 16 Superalloy. J. Mater. Eng. Perform., 19 (2010) 1031-1036.

[18] B.J. Griffiths, Mechanisms of white layer generation with reference to machining and deformation processes. J. Tribol., 109 (1987) 525-530.

[19] N. Narutaki, Y. Yamane, K. Hayashi, T. Kitagawa, K. Uehara, High-speed machining of Inconel 718 with ceramic tools. CIRP Ann. Manuf. Technol., 42 (1993) 103-106.

[20] B. Zou, M. Chen, C. Huang, Q. An, Study on surface damages caused by turning NiCr20TiAl nickel-based alloy. J. Mater. Process. Technol., 209 (2009) 5802-5809.

[21] K.W. Kim, W.Y. Lee, H.C. Sin, A finite-element analysis of machining with the tool edge considered. J. Mater. Process. Technol., 86 (1998) 45-55.

[22] Y. Yen, A. Jain, T. Altan, A finite element analysis of orthogonal machining using different tool edge geometries. J. Mater. Process. Technol., 146 (2004) 72-81.

[23] J.M. Oblak, D.F. Paulonis, D.S. Duvall, Coherency strengthening in Ni-base alloys hardened by DO_{22} gamma double prime precipitates. Metall. Trans., 5 (1974) 143-153.